Ion core structure in $(N_2O)_n^+(n=2-8)$ studied by infrared photodissociation spectroscopy

Yoshiya Inokuchi,[a)] Ryoko Matsushima, Yusuke Kobayashi, and Takayuki Ebata
*Department of Chemistry, Graduate School of Science, Hiroshima University,
Higashi-Hiroshima, Hiroshima 739-8526, Japan*

IR photodissociation (IRPD) spectra of $(N_2O)_2^+ \cdot Ar$ and $(N_2O)_n^+$ with $n=3-8$ are measured in the $1000-2300$ cm^{-1} region. The $(N_2O)_2^+ \cdot Ar$ ion shows an IRPD band at 1154 cm^{-1}, which can be assigned to the out-of-phase combination of the ν_1 vibrations of the N_2O components in the $N_4O_2^+$ ion; the positive charge is delocalized over the two N_2O molecules. The geometry optimization and the vibrational analysis at the $B3LYP/6-311+G^*$ level show that the $N_4O_2^+$ ion has a C_{2h} structure with the oxygen ends of the N_2O components bonded to each other. The IRPD spectra of the $(N_2O)_n^+(n=3-8)$ ions show three prominent bands at ~1170, ~1275, and ~2235 cm^{-1}. The intensity of the ~1170 cm^{-1} band relative to that of the other bands decreases with increasing the cluster size. Therefore, the ~1170 cm^{-1} band is ascribed to the $N_4O_2^+$ dimer ion core and the ~1275 and ~2235 cm^{-1} bands are assigned to the ν_1 and ν_3 vibrations of solvent N_2O molecules, respectively. Since the band of the $N_4O_2^+$ ion core is located at almost the same position for all the $(N_2O)_n^+(n=2-8)$ clusters, the C_{2h} structure of the dimer ion core does not change so largely by the solvation of N_2O molecules, which is quite contrastive to the isoelectronic $(CO_2)_n^+$ case.
© *2009 American Institute of Physics.* [DOI: 10.1063/1.3194801]

I. INTRODUCTION

Ion-molecule complexes play significant roles as reaction intermediates in a number of chemical reactions. For example, the formation of chemical bonds between unsaturated groups such as C=C and C=O with ions is thought to be primary processes of chemical reactions catalyzed by acid and base.[1–3] Because of the importance of ion-molecule complexes in chemical reactions, gas-phase cluster ions have been extensively investigated experimentally and theoretically.[4,5] One of the fundamental issues related to chemical reactions is the identification of the formation of intermolecular covalent bonds in cluster ions. If a covalent bond is formed between an ion and a molecule by the resonance interaction, the charge is delocalized over the complex.

The target systems in this study are the N_2O cluster ions, $(N_2O)_n^+$. This study is an extension of our IR photodissociation (IRPD) studies of $(CS_2)_n^+$ and $(CO_2)_n^+$.[6,7] In these clusters, the intermolecular charge resonance (CR) interaction occurs between two component molecules and provides a symmetrical dimer ion core with an intermolecular covalent bond called "two-center-three-electron bond."[8–33] In the case of $(N_2O)_n^+$, the binding energy of the $(N_2O)_2^+$ ion was estimated as 13.1 kcal/mol from the ionization energies of N_2O and $(N_2O)_2$.[10] This value is comparable to the binding energy of the $(CO_2)_2^+$ ion formed by the CR interaction. Thermochemical measurements with high pressure mass spectrometers also provided the binding energy of the $(N_2O)_2^+$ ion.[18,34] Illies[18] reported a binding energy of 13.3 kcal/mol;

on the basis of the feature of the highest occupied molecular orbital of N_2O, the structure of the $(N_2O)_2^+$ ion was proposed with an intermolecular bond formed between the oxygen ends. The binding energies of the $(N_2O)_n^+$ ions determined by Hiraoka *et al.*[34] were 17.4, 5.7, 5.6, 4.4, and 4.1 kcal/mol for $n=2-6$; they concluded that the $(N_2O)_n^+$ cluster ions have an $(N_2O)_2^+$ dimer ion core with N_2O molecules attached to the ion core. Bowers and co-workers[35] studied dissociation dynamics and energy disposal in the photoexcitation of the $(N_2O)_2^+$ ion in the visible region. They suggested that the photodissociation of the $(N_2O)_2^+$ ion in the visible region occurs by a direct transition to a repulsive potential surface; this surface will be created by the CR interaction between the N_2O components in the $(N_2O)_2^+$ ion. A theoretical study done by McKee[32] showed two types of isomers for the $(N_2O)_2^+$ ion; one is a C_{2h} structure in which the N_2O molecules are bonded at the oxygen ends and the other one is a distorted T-shaped structure. The vibrational structure of the N_2O^+ monomer ion in the electronic ground state was revealed with spectroscopic studies such as Fourier transform emission spectroscopy in the gas phase[36] and IR spectroscopy in solid Ne.[37] However, no spectroscopic study was reported for the $(N_2O)_n^+$ clusters. Nizkorodov and Bieske[38] reported energy disposal in the photodissociation of the $(N_2O)_2^+$ and $(N_2O)_3^+$ ions in the visible region.

In the present study, we investigate the structure of the $(N_2O)_n^+$ ionic clusters $(n=2-8)$ with IRPD spectroscopy. The IRPD spectra are measured in the $1000-2300$ cm^{-1} region and provide IR bands of the symmetric and antisymmetric stretching vibrations $(\nu_1$ and $\nu_3)$ characteristic of an ion core and solvent molecules. In order to obtain the IR spectrum of the $(N_2O)_2^+$ ion, the Ar tagging method is utilized;

―――――――――――――
[a)]Author to whom correspondence should be addressed. Electronic mail:
y-inokuchi@hiroshima-u.ac.jp.

the IRPD spectrum of the $(N_2O)_2{}^+\cdot Ar$ ion is measured while monitoring the Ar loss channel.[39] Since the ionization potential of Ar (15.759 eV) is substantially higher than that of N_2O (12.89 eV), the attachment of an Ar atom is expected not to change so much the positive charge distribution for the $(N_2O)_2{}^+$ ion.[40,41] In order to assign the IRPD spectra, we carry out the geometry optimization and the vibrational analysis of several species at the B3LYP/6-311+G* level of theory. Comparing the IRPD spectra with calculated ones, we discuss the ion core form existing in the $(N_2O)_n{}^+$ clusters.

II. EXPERIMENTAL AND COMPUTATIONAL

The details of our experiment have been given in our previous report.[6] For IRPD spectroscopy of the $(N_2O)_n{}^+$ (n =3−8) ions, pure N_2O gas is injected into a source chamber through a pulsed nozzle (General Valve Series 9) with a stagnation pressure of 0.2 MPa. In the case of the $(N_2O)_2{}^+\cdot Ar$ ion, a gas mixture of $N_2O(\sim1\%)$ and Ar is used with a pressure of 0.8 MPa. The pulsed free jet crosses an electron beam at the exit of the nozzle with an electron kinetic energy of 350 eV, producing $(N_2O)_n{}^+$ and $(N_2O)_n{}^+\cdot Ar$. Cluster ions produced are accelerated into a flight tube by applying pulsed electric potential (~1.3 kV) to Wiley–McLaren type acceleration grids. In the flight tube, only target parent ions can go through a mass gate. After passing through the gate, mass-selected parent ions are merged with an output of a pulsed IR laser. Resultant fragment ions are mass analyzed by a home-made reflectron mass spectrometer and detected by a multichannel plate (MCP) (Burle 31373). An output from the MCP is amplified by a commercial amplifier (Stanford Research Systems SR445A) and fed into a digital storage oscilloscope (LeCroy 9310A). A signal averaged by the oscilloscope is transferred to a computer through the general purpose interface bus (GPIB) interface. Yields of fragment ions are normalized by the intensity of parent ions and the photodissociation laser. IRPD spectra of parent ions are obtained by plotting normalized yields of fragment ions against the wavenumber of the IR laser. The fragmentation channel detected for the IRPD spectra of the $(N_2O)_n{}^+$ ions and the $(N_2O)_2{}^+\cdot Ar$ ion is the loss of one N_2O molecule and the Ar atom, respectively.

The tunable IR light used in this study is obtained by difference frequency generation (DFG) between a signal and an idler output of an optical parametric oscillator (OPO) (LaserVision). The OPO laser is pumped by a fundamental output of a Nd:YAG (neodymium-doped yttrium aluminum garnet) laser (Spectra Physics GCR250). A AgGaSe$_2$ crystal is used for DFG and only the DFG output is introduced to the vacuum chamber after the signal and idler outputs are removed with a ZnSe filter. The power of the IR laser is measured with a laser detector (Ophir 12A-P). The output energy is 0.2–1 mJ/pulse in the 1100–2300 cm^{-1} region.

In order to analyze IRPD spectra, we also carry out density functional theory (DFT) calculations with the GAUSSIAN03 program package.[42] The geometry optimization and the vibrational analysis of N_2O, N_2O^+, $(N_2O)_2{}^+$, and $(N_2O)_3{}^+$ are done at the B3LYP/6-311+G* level of theory. For comparison of the IRPD spectra with calculated ones, a scaling
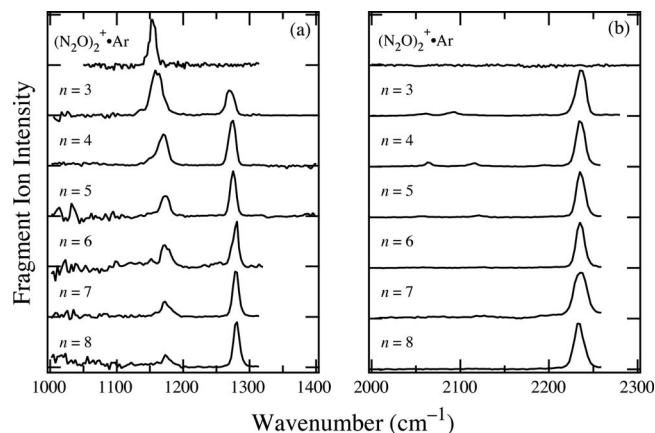
FIG. 1. The IRPD spectra of $(N_2O)_2{}^+\cdot Ar$ and $(N_2O)_n{}^+$ (n=3–8) in the ν_1 (a) and the ν_3 (b) regions. Intensity of the fragment ion for each spectrum is normalized with the maximum value.

factor of 0.9588 is employed to vibrational frequencies calculated. This factor is determined so as to reproduce the frequency of the symmetric stretching (ν_1) and the antisymmetric stretching (ν_3) vibrations of neutral N_2O monomer.[43]

III. RESULTS AND DISCUSSION

A. IRPD spectra

Figures 1(a) and 1(b) show the IRPD spectra of $(N_2O)_n{}^+$ in the ν_1 and ν_3 regions, respectively. For the n=2 ion, the IRPD spectrum of the $(N_2O)_2{}^+\cdot Ar$ ion is shown in Fig. 1. The $(N_2O)_2{}^+$ ion is not photodissociated in this frequency region, suggesting that the $(N_2O)_2{}^+$ ion has an intermolecular binding energy substantially larger than those of higher clusters. In the spectrum of $(N_2O)_2{}^+\cdot Ar$, only one band is observed at 1154 cm^{-1} and no strong band is found in the ν_3 region. For the $(N_2O)_3{}^+$ ion, three strong bands can be seen at 1160, 1270, and 2236 cm^{-1}. In addition, very weak bands are seen at around 2100 cm^{-1}. The IRPD spectra of the clusters larger than n=3 also show three bands at ~1170, ~1275, and ~2235 cm^{-1}. The intensity of the 1275 cm^{-1} band relative to that of the 1170 cm^{-1} one increases with increasing the cluster size. Neutral N_2O monomer has the ν_1 and ν_3 vibrations at 1285.0 and 2223.5 cm^{-1}, respectively.[43] Therefore, the ~1275 and ~2235 cm^{-1} bands of the n =3−8 ions can be assigned to the ν_1 and ν_3 vibrations of solvent N_2O molecules, respectively. The bands at around 1170 cm^{-1} of the n=2−8 ions are ascribed to an ion core in the clusters. The position of the ion core band is almost the same for all the $(N_2O)_n{}^+$ (n=2−8) clusters, indicating that these clusters have a common ion core species. In the IRPD spectrum of the $(N_2O)_2{}^+\cdot Ar$ ion, no band assignable to a solvent N_2O molecule is observed at around 1275 cm^{-1}. Therefore, the ~1170 cm^{-1} bands of the $(N_2O)_n{}^+$ ions can be attributed to the ν_1 vibration of the $N_4O_2{}^+$ ion core, in which the positive charge is delocalized over the two N_2O molecules. As can be seen in Fig. 1(a), the intensity of the $N_4O_2{}^+$ band is comparable to that of the solvent N_2O molecule in the ν_1 region. In the ν_3 region, however, there is no
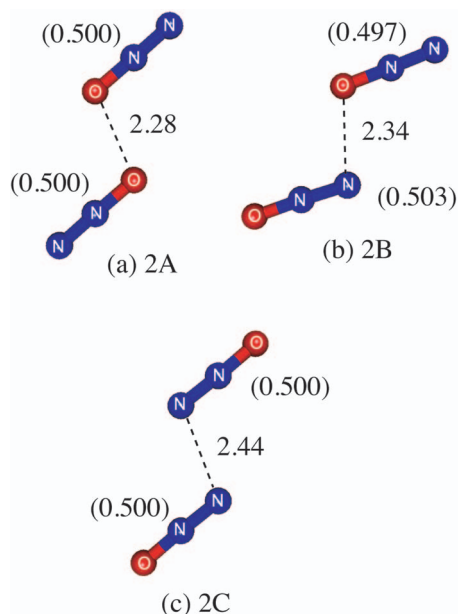
FIG. 2. The optimized structure of the $(N_2O)_2^+$ ion calculated at the B3LYP/6-311+G* level of theory. Numbers in the figure are the distance of the intermolecular bond drawn with dotted lines in angstroms. Numbers in parentheses represent the charge distribution in constituent molecules. All the structures in the figure have a planar form.

strong band assignable to the $N_4O_2^+$ ion core [Fig. 1(b)]. The ν_3 band of the $N_4O_2^+$ ion core may probably be quite weaker than that of the solvent N_2O molecule.

B. Structure of $(N_2O)_2^+$

The IRPD results suggest that the $(N_2O)_n^+(n=2-8)$ cluster ions have an $N_4O_2^+$ ion core. In order to determine the structure of the ion core, we carried out the geometry optimization and the vibrational analysis of the $(N_2O)_2^+$ ion at the B3LYP/6-311+G* level of theory. Figure 2 shows the optimized structure of the $(N_2O)_2^+$ ion. In all the three stable isomers (2A–2C), the positive charge is delocalized over the

two constituent molecules, described as $N_4O_2^+$. The relative energy, binding energy, vibrational frequency, IR intensity, and vibrational mode of the $N_4O_2^+$ isomers are collected in Table I. Isomer 2A is the most stable structure, in which two N_2O components are connected at the oxygen ends. The second most stable isomer is 2B; the intermolecular bond is formed between the oxygen and the nitrogen ends. In isomer 2C, the nitrogen ends are bonded to each other. Isomers 2A and 2C have C_{2h} symmetry and isomer 2B has a planar C_s structure. As shown in Fig. 2, the more stable the $N_4O_2^+$ isomer, the shorter the intermolecular bond. In Fig. 3, the IRPD spectrum of the $(N_2O)_2^+\cdot Ar$ ion is compared with the IR spectra of isomers 2A–2C. Isomers 2A–2C exhibit quite different IR spectra from each other. Isomer 2A has two IR bands at 1178 and 2087 cm^{-1}. These bands are the out-of-phase combinations of the ν_1 and ν_3 vibrations, respectively.[7] The in-phase combinations are IR inactive in C_{2h} symmetry and do not emerge in the IR spectrum of 2A.[7] Isomer 2C also has the ν_1 and ν_3 bands at 1287 and 2041 cm^{-1}. In the case of isomer 2B, there are two bands for each of the ν_1 and ν_3 vibrations. The IRPD spectrum of the $(N_2O)_2^+\cdot Ar$ ion displays one strong band at 1154 cm^{-1}. This band position agrees better with those predicted for 2A (1178 cm^{-1}) and 2B (1172 cm^{-1}) than with that for 2C (1287 cm^{-1}). Isomer 2B has another ν_1 band at 1291 cm^{-1}. However, the IRPD spectrum does not show any band around 1290 cm^{-1}. Therefore, the structure of the $N_4O_2^+$ ion core in the $(N_2O)_2^+\cdot Ar$ ion can be attributed to isomer 2A. The IRPD spectrum of the $(N_2O)_2^+\cdot Ar$ ion does not show strong absorption in the ν_3 (2000–2300 cm^{-1}) region, suggesting that the ν_3 band is weaker than the ν_1 band for the $N_4O_2^+$ ion core. This tendency for the relative intensity of the ν_1 and ν_3 bands also agrees with that of 2A; the ν_1 band is stronger than the ν_3 one for 2A, whereas the former band is weaker than the latter for 2B and 2C. Though the attachment of the Ar atom to isomer 2A may lower the overall symmetry of the $(N_2O)_2^+\cdot Ar$ ion, the IRPD spectrum of the $(N_2O)_2^+\cdot Ar$ ion exhibits only the out-of-phase combination band in the ν_1

TABLE I. Relative energies, binding energies, vibrational frequencies, IR intensities, and vibrational modes for optimized isomers of $N_4O_2^+$ at the B3LYP/6-311+G* level.

Isomer	Relative energy[a] (cm^{-1})	Binding energy[a,b] (cm^{-1})	Frequency[c] (cm^{-1})	IR intensity ($km\ mol^{-1}$)	Vibrational modes[d]
2A	(0)	10936	1165	0 (a_g)	ν_1 (ip)
(C_{2h})			1178	144 (b_u)	ν_1 (oop)
			2079	0 (a_g)	ν_3 (ip)
			2087	49 (b_u)	ν_3 (oop)
2B	679	10257	1172	73 (a')	ν_1
(Cs)			1291	13 (a')	ν_1
			2027	204 (a')	ν_3
			2089	37 (a')	ν_3
2C	1363	9572	1287	24 (b_u)	ν_1 (oop)
(C_{2h})			1295	0 (a_g)	ν_1 (ip)
			2016	0 (a_g)	ν_3 (ip)
			2041	483 (b_u)	ν_3 (oop)

[a]The correction with the zero-point vibrational energy is performed to obtain these values.
[b]The fragment species are N_2O^+ and N_2O.
[c]A scaling factor of 0.9588 is employed for the calculated frequencies.
[d]"oop" and "ip" stand for the out-of-phase and in-phase combinations of the ν_1 and ν_3 vibrations.
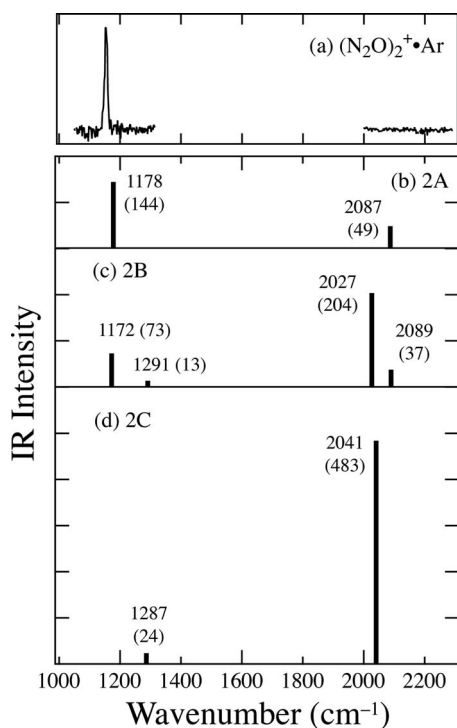
FIG. 3. (a) The IRPD spectrum of $(N_2O)_2{}^+\cdot Ar$. [(b)–(d)] The IR spectra calculated for isomers 2A–2C at the B3LYP/6-311+G* level of theory. Numbers in the figure show the vibrational frequency in cm^{-1} unit. The IR intensity of the vibrations in km/mol unit is displayed in parentheses.

FIG. 4. (a) The IRPD spectrum of $(N_2O)_3{}^+$. (b) The summation of the calculated IR spectra of neutral N_2O and isomer 2A. [(c)–(e)] The IR spectra calculated for neutral N_2O, isomer 2A, and the most stable isomer of $(N_2O)_3{}^+$ (isomer 3A) at the B3LYP/6-311+G* level of theory. Numbers in Fig. 4(c) show the vibrational frequency in cm^{-1} unit. The IR intensity of the vibrations in km/mol unit is displayed in parentheses in Fig. 4(c). The solid curves are the IR spectra reproduced by using Lorentzian components with a full width at half maximum of 20 cm^{-1}. The structure of isomer 3A is shown in Fig. 4(e); numbers in parentheses are the charge distribution in each of the component molecules.

region. This result indicates that the Ar atom in the $(N_2O)_2{}^+\cdot Ar$ ion hardly affects the planar structure of the $N_4O_2{}^+$ ion core. The $(N_2O)_2{}^+\cdot Ar$ ion acts as a C_{2h} symmetry species for the IR absorption of the $N_4O_2{}^+$ ion part.

C. Structure of $(N_2O)_n{}^+(n=3-8)$

Similar to the case of $(CS_2)_3{}^+$ and $(CO_2)_3{}^+$, the DFT calculations of the $(N_2O)_3{}^+$ ion provide only isomers in which the positive charge is delocalized over the three components; these calculation results seem inconsistent with the IRPD result of the $(N_2O)_3{}^+$ ion that the bands assignable to the solvent N_2O molecule appear at 1270 and 2236 cm^{-1}.[6,7] In Fig. 4, the IRPD spectrum of the $(N_2O)_3{}^+$ ion is displayed with the IR spectra calculated for neutral N_2O monomer, isomer 2A, and the most stable isomer of the $(N_2O)_3{}^+$ ion (isomer 3A). The solid curves in Figs. 4(c)–4(e) are the IR spectra reproduced by providing Lorentzian components with a full width at half maximum of 20 cm^{-1} for the calculated IR bands. Figure 4(b) represents the sum of the reproduction curves of neutral N_2O monomer [Fig. 4(c)] and isomer 2A [Fig. 4(d)]. The structure of isomer 3A is also shown in Fig. 4(e); it has a planar C_s structure and the positive charge is delocalized over the three N_2O components. The IRPD spectrum of the $(N_2O)_3{}^+$ ion has three strong bands at 1160, 1270, and 2236 cm^{-1} with very weak maxima at ~ 2095 and ~ 2060 cm^{-1}. The calculated IR spectrum of neutral N_2O shows the ν_3 band at 2247 cm^{-1}, which is substantially stronger than the ν_1 band at 1272 cm^{-1} and the 1178 and 2087 cm^{-1} bands of isomer 2A. The position and the relative intensity of the IRPD bands of $(N_2O)_3{}^+$ [Fig. 4(a)] agree well with those of the sum spectrum in Fig. 4(b).

In addition, the spectral feature of isomer 3A [Fig. 4(e)] does not correspond with that of the IRPD spectrum of the $(N_2O)_3{}^+$ ion [Fig. 4(a)]. Therefore, it is concluded that the $(N_2O)_3{}^+$ ion in the experiment has a $N_4O_2{}^+$ ion core with the structure of isomer 2A and a solvent N_2O molecule. The weak 2095 cm^{-1} component of the IRPD spectrum of $(N_2O)_3{}^+$ can be assigned to the ν_3 band of the $N_4O_2{}^+$ ion core. The ν_3 band of the solvent N_2O molecule at 2236 cm^{-1} is substantially stronger than that of the $N_4O_2{}^+$ ion core at 2095 cm^{-1} in the IRPD spectrum of the $(N_2O)_3{}^+$ ion. This intensity inequality is consistent with the prediction based on the IRPD result of the $(N_2O)_2{}^+ Ar$ ion that the ν_3 band is not clearly found at around 2100 cm^{-1} [Fig. 3(a)]. The weak hump at 2060 cm^{-1} may originate from other $N_4O_2{}^+$ ion cores like 2B and 2C, although it is quite minor in the experiment. As seen in Fig. 1(a), since the band position of the $N_4O_2{}^+$ ion core in the ν_1 region is similar for the $(N_2O)_n{}^+(n=2-8)$ ions, all the $(N_2O)_n{}^+$ ions has the $N_4O_2{}^+$ ion core like isomer 2A. Strictly speaking, however, the IRPD bands of the dimer ion core at around 1160 cm^{-1} show the band shift with increasing the cluster size. The band positions are 1154, 1160, 1169, 1173, 1173, 1174, and 1174 cm^{-1} for the $n=2-8$ ions; the bands move largely for up to $n=4$. This band shift may probably be characteristic of the solvation around the dimer ion core. The first and the second solvent N_2O molecules are bonded to the dimer ion

core tightly, resulting in the large band shift for up to $n=4$. Since the third to sixth solvent N$_2$O molecules are weakly bound to the dimer ion core, the band position does not change so much for $n=4$–8. This trend of the band position agrees with the results of the thermochemical measurements of the $(N_2O)_n^+$ ions done by Hiraoka *et al.*;[34] the binding energy of the $(N_2O)_n^+$ ions shows irregular decrease between $n=4$ and 5 ions.

Here it is of interest to compare the structure of the $(N_2O)_n^+$ cluster ions with that of isoelectronic $(CO_2)_n^+$ cluster ions. As mentioned above, the $N_4O_2^+$ ion core keeps the C_{2h} form against the solvation of N$_2$O molecules. In contrast, the $(CO_2)_n^+$ ions show alternate change in the IR absorption for the $C_2O_4^+$ ion core as a function of the cluster size. This spectral change is ascribed to the structural deformation of the $C_2O_4^+$ ion core part.[7] The $(CO_2)_3^+$ and $(CO_2)_5^+$ ions show two IRPD bands of the $C_2O_4^+$ ion core in the antisymmetric CO stretching region, indicating that the $C_2O_4^+$ ion core has a symmetry lower than C_{2h}. In the case of the $(CO_2)_4^+$ and $(CO_2)_n^+(n=6$–8) ions, there is only one IRPD band; the ion core regains a C_{2h} form.

One possible origin for the difference in the structural change is that the rigidity of the C_{2h} form is different between $N_4O_2^+$ and $C_2O_4^+$. Figure 5(a) shows potential energy surfaces (PESs) of the $N_4O_2^+$ (open circles) and $C_2O_4^+$ (closed circles) ions as a function of the dihedral angle of atoms 2–3–4–5 calculated at the B3LYP/6-311+G* level. Numbering of the atoms in $N_4O_2^+$ and $C_2O_4^+$ is presented in Fig. 5. The steepness of the PES of the $N_4O_2^+$ ion is similar to that of the $C_2O_4^+$ one, meaning that the rigidity of the planar form is almost the same for $N_4O_2^+$ and $C_2O_4^+$. In the calculations of the PESs, we also perform the vibrational analysis for each of the optimized structures; it may probably be helpful to examine the IR spectral feature with the change in the intermolecular coordinates of the clusters, so far as high-frequency, intramolecular vibrations are concerned. The IR intensity of the in-phase combination relative to that of the out-of-phase one for the ν_1 vibration of $N_4O_2^+$ and the ν_3 vibration of $C_2O_4^+$ are shown in Fig. 5(b). At the dihedral angle of 180°, the relative IR intensity is calculated to be zero for $N_4O_2^+$ and $C_2O_4^+$. The curve of the ν_1 vibration of $N_4O_2^+$ is quite similar to that of the ν_3 vibration of $C_2O_4^+$ in the 100°–260° degree region; the sensitivity of the relative IR intensity to the deformation of the planar form is almost the same for $N_4O_2^+$ and $C_2O_4^+$. Therefore, no considerable difference is found for the property of the structure and the IR absorption of $N_4O_2^+$ and $C_2O_4^+$.

The other possible reason for the difference between $(N_2O)_n^+$ and $(CO_2)_n^+$ is the strength of the intermolecular interaction between the dimer ion core and the solvent molecules. Though N$_2$O has dipole moment, it is quite small (0.16 D).[44] In addition, the polarizability is similar between N$_2$O $(3.03 \times 10^{-24}$ cm^3) and CO$_2$ $(2.91 \times 10^{-24}$ cm^3).[44] Therefore, the electrostatic interaction between the dimer ion core and the solvent molecules is expected to be comparable for $(N_2O)_n^+$ and $(CO_2)_n^+$. One noticeable difference between $(N_2O)_n^+$ and $(CO_2)_n^+$ is the binding energy of the dimer ion. The binding energy of the $N_4O_2^+$ ion (isomer 2A) is estimated as 10 936 cm^{-1} at the B3LYP/6-311+G* level. The
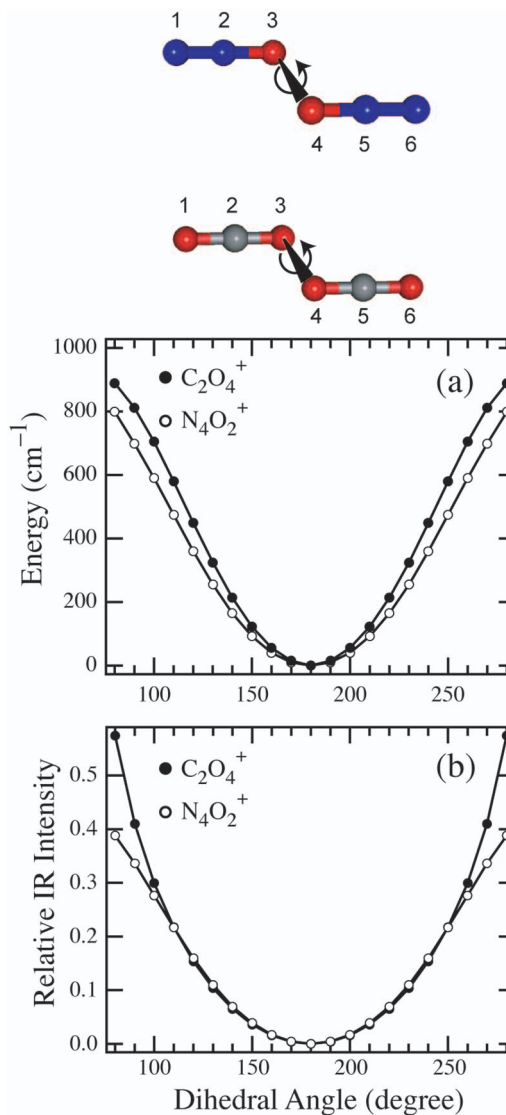
FIG. 5. (a) The PES of the $N_4O_2^+$ (open circles) and $C_2O_4^+$ (closed circles) ions as a function of the dihedral angle of atoms 2–3–4–5. The calculations are performed at the B3LYP/6-311+G* level of theory. To obtain these PESs, the dihedral angle is fixed and all the other degrees of freedom are optimized with an interval of 10°. (b) The IR intensity of the in-phase combination relative to that of the out-of-phase one for the ν_1 vibration of $N_4O_2^+$ (open circles) and the ν_3 vibration of $C_2O_4^+$ (closed circles) as a function of the dihedral angle. The vibrational analysis is carried out for each of the optimized structures at the B3LYP/6-311+G* level of theory.

calculation of the $C_2O_4^+$ ion at the same level predicts 10 283 cm^{-1}, smaller than that of $N_4O_2^+$. The thermochemical measurements done by Hiraoka *et al.*[17,34] showed 17.4 and 15.6 kcal/mol for the binding energy of $N_4O_2^+$ and $C_2O_4^+$, respectively. The smaller binding energy of $C_2O_4^+$ than that of $N_4O_2^+$ suggests a smaller difference in the ionization potential between C_2O_4 and CO$_2$ than that between N_4O_2 and N$_2$O. The smaller difference in the ionization potential may result in the charge transfer from the dimer ion core to solvent molecules more for the $C_2O_4^+ \bullet \bullet \bullet (CO_2)_{n-2}$ system than for the $N_4O_2^+ \bullet \bullet \bullet (N_2O)_{n-2}$ system. As a result, the deformation of the ion core may probably occur only for the $(CO_2)_n^+$ clusters. A theoretical examination of the intermolecular interaction in $(N_2O)_n^+$ and $(CO_2)_n^+$ is required for the determination of the cluster structure.

IV. SUMMARY

The IRPD spectra of $(N_2O)_2^+ \cdot Ar$ and $(N_2O)_n^+$ with $n = 3-8$ were measured in the $1000-2300$ cm^{-1} region. The IRPD bands at ~ 1170 cm^{-1} for the $n = 2-8$ clusters are assigned to the $N_4O_2^+$ ion core. The IRPD spectra of the $(N_2O)_n^+$ ($n = 3-8$) ions show the bands at ~ 1275 and ~ 2235 cm^{-1} in addition to the $N_4O_2^+$ band. These bands are attributed to the ν_1 and ν_3 vibrations of solvent N_2O molecules. The geometry optimization and the vibrational analysis at the B3LYP/6-311+G* level show that the $N_4O_2^+$ ion has a C_{2h} structure with the oxygen ends of the N_2O components bonded to each other. Since the band position of the $N_4O_2^+$ ion core is similar for all the $(N_2O)_n^+$ ($n = 2-8$) ions, the C_{2h} structure of the dimer ion core does not change much through solvation by N_2O molecules. These $(N_2O)_n^+$ results are quite contrastive to that of the isoelectronic $(CO_2)_n^+$ clusters. We propose that the charge transfer from the dimer ion core to solvent molecules can cause the noticeable structural change for the $C_2O_4^+$ ion core in the $(CO_2)_n^+$ clusters.

ACKNOWLEDGMENTS

[1] S. H. Pine, *Organic Chemistry*, 5th ed. (McGraw-Hill, Singapore, 1987).
[2] J. McMurry, *Organic Chemistry*, 5th ed. (Brooks/Cole, California, 2000).
[3] M. B. Smith and J. March, *MARCH'S Advanced Organic Chemistry: Reactions, Mechanisms, and Structure*, 5th ed. (Wiley, New York, 2001), Chap. 16.
[4] A. W. Castleman, Jr., and R. G. Keesee, Acc. Chem. Res. **19**, 413 (1986).
[5] A. W. Castleman, Jr., and K. H. Bowen, Jr., J. Phys. Chem. **100**, 12911 (1996).
[6] Y. Kobayashi, Y. Inokuchi, and T. Ebata, J. Chem. Phys. **128**, 164319 (2008).
[7] Y. Inokuchi, A. Muraoka, T. Nagata, and T. Ebata, J. Chem. Phys. **129**, 044308 (2008).
[8] M. Meot-Ner (Mautner) and F. H. Field, J. Chem. Phys. **66**, 4527 (1977).
[9] G. G. Jones and J. W. Taylor, J. Chem. Phys. **68**, 1768 (1978).
[10] S. H. Linn and C. Y. Ng, J. Chem. Phys. **75**, 4921 (1981).
[11] K. Stephan, J. H. Futrell, K. I. Peterson, A. W. Castleman, Jr., and T. D. Märk, J. Chem. Phys. **77**, 2408 (1982).
[12] J. V. Headley, R. S. Mason, and K. R. Jennings, J. Chem. Soc., Faraday Trans. 1 **78**, 933 (1982).
[13] P. A. M. van Koppen, P. R. Kemper, A. J. Illies, and M. T. Bowers, Int. J. Mass Spectrom. Ion Process. **54**, 263 (1983).
[14] G. Romanowski and K. P. Wanczek, Int. J. Mass Spectrom. Ion Process. **62**, 277 (1984).
[15] G. Romanowski and K. P. Wanczek, Int. J. Mass Spectrom. Ion Process. **70**, 247 (1986).
[16] P. C. Engelking, J. Chem. Phys. **87**, 936 (1987).
[17] K. Hiraoka, G. Nakajima, and S. Shoda, Chem. Phys. Lett. **146**, 535 (1988).
[18] A. J. Illies, J. Phys. Chem. **92**, 2889 (1988).
[19] C. Praxmarer, A. Hansel, A. Jordan, H. Kraus, and W. Lindinger, Int. J. Mass Spectrom. Ion Process. **129**, 121 (1993).
[20] B. R. Cameron, C. G. Aitken, and P. W. Harland, J. Chem. Soc., Faraday Trans. **90**, 935 (1994).
[21] G. P. Smith and L. C. Lee, J. Chem. Phys. **69**, 5393 (1978).
[22] A. J. Illies, M. F. Jarrold, W. Wagner-Redeker, and M. T. Bowers, J. Phys. Chem. **88**, 5204 (1984).
[23] M. A. Johnson, M. L. Alexander, and W. C. Lineberger, Chem. Phys. Lett. **112**, 285 (1984).
[24] M. L. Alexander, M. A. Johnson, and W. C. Lineberger, J. Chem. Phys. **82**, 5288 (1985).
[25] H.-S. Kim, M. F. Jarrold, and M. T. Bowers, J. Chem. Phys. **84**, 4882 (1986).
[26] P. C. Engelking, J. Chem. Phys. **85**, 3103 (1986).
[27] M. E. Jacox and W. E. Thompson, J. Chem. Phys. **91**, 1410 (1989).
[28] M. Zhou and L. Andrews, J. Chem. Phys. **110**, 6820 (1999).
[29] W. E. Thompson and M. E. Jacox, J. Chem. Phys. **111**, 4487 (1999).
[30] I. A. Shkrob, M. C. Sauer, Jr., C. D. Jonah, and K. Takahashi, J. Phys. Chem. A **106**, 11855 (2002).
[31] A. J. Illies, M. L. McKee, and H. Bernhard Schlegel, J. Phys. Chem. **91**, 3489 (1987).
[32] M. L. McKee, Chem. Phys. Lett. **165**, 265 (1990).
[33] I. A. Shkrob, J. Phys. Chem. A **106**, 11871 (2002).
[34] K. Hiraoka, S. Fujimaki, K. Aruga, T. Sato, and S. Yamabe, J. Chem. Phys. **101**, 4073 (1994).
[35] L. Misev, A. J. Illies, M. F. Jarrold, and M. T. Bowers, Chem. Phys. **95**, 469 (1985).
[36] E. Fellows and M. Vervloet, Chem. Phys. **264**, 203 (2001).
[37] E. Jacox, J. Chem. Phys. **93**, 7622 (1990).
[38] S. A. Nizkorodov and E. J. Bieske, Chem. Phys. **239**, 369 (1998).
[39] M. Okumura, L. I. Yeh, J. D. Myers, and Y. T. Lee, J. Chem. Phys. **85**, 2328 (1986).
[40] K. Kimura, S. Katsumata, Y. Achiba, T. Yamazaki, and S. Iwata, *Handbook of HeI Photoelectron Spectra of Fundamental Organic Molecules* (Japan Scientific Societies, Tokyo, 1981).
[41] The NIST Chemistry WebBook, http://webbook.nist.gov/chemistry/.
[42] J. Frisch, G. W. Trucks, H. B. Schlegel, *et al.*, GAUSSIAN03, Gaussian, Inc., Pittsburgh PA, 2003.
[43] G. Herzberg, *Molecular Spectra and Molecular Structure: Infrared and Raman Spectra of Polyatomic Molecules* (Krieger, Malabar, 1991), Vol. 2.
[44] D. R. Lide, *CRC Handbook of Chemistry and Physics*, 82th ed. (CRC, Boca Raton, 2001).